Journal Pre-proofs

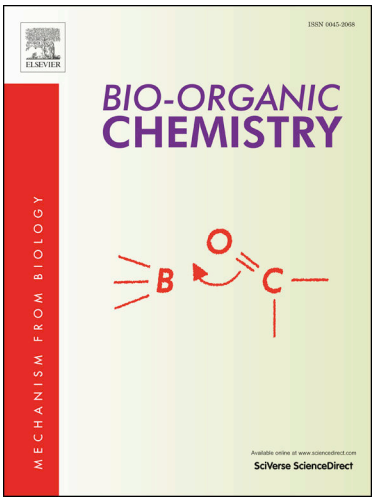

New Cyanopyridine-Based Scaffold as PIM-1 Inhibitors and Apoptotic Inducers: Synthesis and SARs Study

Amel M. Farrag, Mona H. Ibrahim, Ahmed B.M. Mehany, Magda M.F. Ismail

PII: S0045-2068(20)31676-X
DOI: https://doi.org/10.1016/j.bioorg.2020.104378
Reference: YBIOO 104378

To appear in: *Bioorganic Chemistry*

Received Date: 29 June 2020
Revised Date: 24 September 2020
Accepted Date: 4 October 2020

Please cite this article as: A.M. Farrag, M.H. Ibrahim, A.B.M. Mehany, M.M.F. Ismail, New Cyanopyridine-Based Scaffold as PIM-1 Inhibitors and Apoptotic Inducers: Synthesis and SARs Study, *Bioorganic Chemistry* (2020), doi: https://doi.org/10.1016/j.bioorg.2020.104378

New Cyanopyridine-Based Scaffold as PIM-1 Inhibitors and Apoptotic Inducers: Synthesis and SARs Study

Amel M. Farrag,[a*] Mona H. Ibrahim,[a] Ahmed B. M. Mehany[b] and Magda M. F. Ismail[a]

[a] Department of Pharmaceutical Chemistry, Faculty of Pharmacy (Girls), Al-Azhar University, Cairo, Egypt.
[b] Department of Zoology, Faculty of Science (Boys), Al-Azhar University, Cairo, Egypt.

ABSTRACT

Two novel series of 6-(4-benzamido-/4-phthalimido)-3-cyanopyridine derivatives were designed and synthesized as inhibitors of PIM-1 kinase. Based on cytotoxicity results via MTT assay against prostate carcinoma PC3, human hepatocellular carcinoma HepG2 and breast adenocarcinoma MCF-7 cell lines, the most potent cytotoxic cyanopyridine hits, **6**, **7**, **8**, **12** and **13** were 1.5-3.3 times more inhibitor of cell proliferation than the reference standard, 5-FU. Selectivity profile of the latter compounds on normal human cells (WI-38), was executed, indicating that they are highly selective (IC_{50}>145 μM) in their cytotoxic effect. The promising compounds were further evaluated as PIM-1 kinase inhibitors. These compounds elicited remarkable inhibition of PIM-1 kinase (76.43-53.33%). Extensive studies on apoptosis were conducted for these compounds; they enhanced caspase-3 and boosted the Bax/Bcl-2 ratio 27-folds in comparison to the control. Molecular docking study of the most potent compound, **13** in PIM-1 kinase active site was consistent with the *in vitro* activity. Finally, prediction of chemo-informatic properties released compound **13** as the most promising ligand.

Keywords: Synthesis, Cyanopyridine, PIM-1 kinase, Cell cycle analysis, Apoptosis, Docking

1. Introduction:

PIM kinases, the proviral integration site for Moloney murine leukemia virus, are involved in many biological processes such as cell survival, proliferation, differentiation, migration, metabolism, and apoptosis. [1–7] PIM-1 kinase High levels are correlated with many types of cancer such as myeloid leukemia, breast cancer and prostatic cancer, [8–11] while the deficiency of PIM-1 kinase leads to the failure in cell survival and growth. [9,12,13] The identification of PIM-1 role in controlling the growth of cancer stem cells and promotion of multiple drug resistance added more to the importance of developing potent PIM-1 inhibitors as anticancer agents that can defeat the drug resistance created by cancer stem cells.[10,14] Besides, PIM-1 was reported to act as a positive regulator of cell cycle progression at G1/S and G2/M

transitions.[15,16] Activation of caspases plays a central role in the execution phase of cell apoptosis. Caspase 3 activation is required for apoptosis induction in response to chemotherapeutic drugs e.g., taxanes, 5-fluorouracil, and doxorubicin. One of the main regulators of cell survival is the B-cell lymphoma-2 (Bcl-2) family comprising Bcl-2, Bcl-xL and myeloid cell leukaemia-1 (MCL-1). [17]

Inspired by these findings, and as a continuation of our previous work on PIM-1 inhibitors, [18] the goal of this study was to design new PIM-1 kinase inhibitors; through modification of 6-aryl moiety of the reported PIM-1 inhibitor, 6-(5-bromo-2-hydroxy) phenyl-2-oxo-4-phenyl-3-pyridine carbonitrile (VRV). Modification of 6-aryl moiety was achieved via molecular extension using 6-benzamidophenyl and/ rigidification by incorporation of 6-phthalimidophenyl in pyridine core. Moreover, enhancing the cytotoxic potential of the designed compounds was considered via synthesis of cyanopyridine derivatives bearing hydrophilic / hydrophobic moieties at p-4, and bioisosteric replacement at p-2 of pyridine core with OH/NH_2 functionality to explore the impact of structural variation on the anticancer activity. Accordingly, two series of novel cyanopyridines were synthesized and screened via MTT assay for cytotoxic activities against three cancer cell lines, PC-3, HepG-2, and MCF-7 and normal Human cell line WI-38. Then, evaluation of PIM-1 inhibition will be performed. Finally, the promising hits will be tested for apoptosis induction via cell cycle analysis and this study will be substantiated by evaluation of their effect on BAX, Bcl-2 genes and the crucial mediator for programmed cell death, caspase 3.

2. Results and discussion

2.1. Chemistry

Synthesis of two cyanopyridines series were accomplished in scheme **1**. 4-Benzamidoacetophenone **2** was obtained according to the literature [19] by benzoylation of 4-aminoacetophenone with benzoyl chloride in DMF/Stirr. Cyclocondensation of **2** with malononitrile/NH_4OAc [20] was carried out to yield the novel 4-aryl-2-amino-6-(4-benzamidophenyl)-3-cyanopyridines, **3-5**; or with ethyl cyanoacetate by the same reaction condition to give 4-aryl-6-(4-benzamidophenyl)-3-cyanopyridin-2-ones, [21] **6-8; (Scheme 1).**

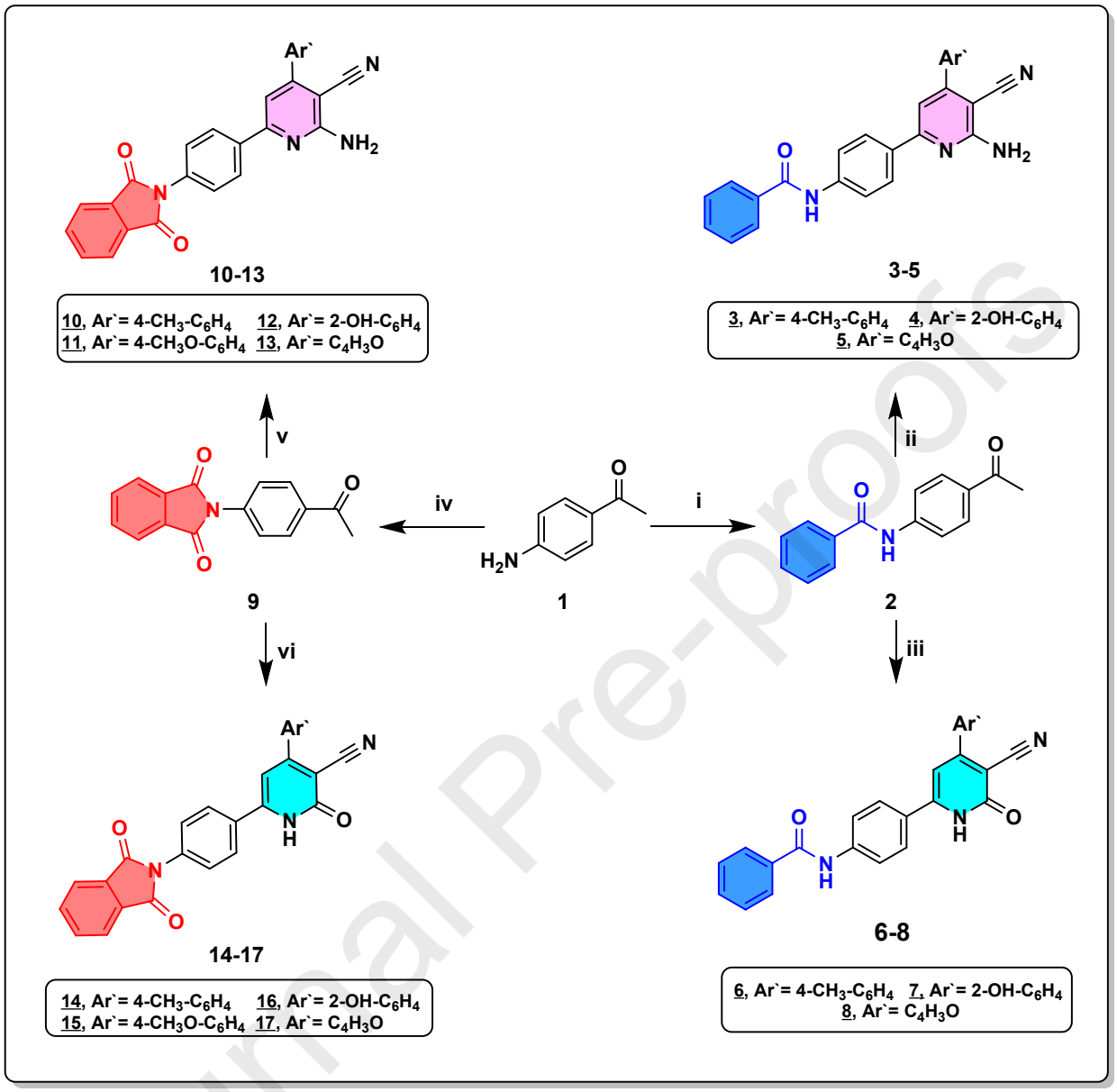

Reagents and conditions: i) C_6H_5COCl, DMF, Et_3N / 0°C, stir, 3h; **ii)** Malononitrile, Ar`-CHO, $NH_4OAC$, EtOH, reflux, 6-8h; **iii)** Ethylcyanoacetate, Ar`-CHO, EtOH, NH_4OAC, reflux, 4-6 h; **iv) Phthalic anhydride**, ACOH, reflux, 4h; **v)** Malononitrile, Ar`-CHO, $NH_4OAC$, ACOH, reflux, 12h; **vi)** Ethylcyanoacetate, Ar`-CHO, ACOH, NH_4OAC, reflux, 12h.

Scheme 1: Synthesis of the target cyanopyridine derivatives **3-8** and **10-17**.

The structures of all 6-(4-benzamidophenyl) series, **3-8** were assigned by spectral data and elemental analysis. Thus, IR spectrum of **3** (as an example) showed strong absorption bands at 3345 and 3300 cm^{-1} attributed to the NH_2 and NH groups and at 2198 and 1650 cm^{-1} comprising the nitrile and carbonyl of amide groups, respectively. Moreover, ^1H NMR spectrum of **3** revealed a characteristic singlet at δ 2.38 ppm representing methyl protons. Also, the pyridine proton appeared at δ 7.10 ppm as a singlet signal.

On the other hand, nucleophilic substitution reaction of 4-amino-acetophenone and phthalic anhydride produced another intermediate, 2-(4-acetylphenyl) isoindoline-1,3-dione, **9.** [22] Similarly, cyclocondensation of **9** with malononitrile or ethyl cyanoacetate in NH_4OAc [23] was afforded to give both 2-amino-4-aryl-6-(4-phthalimidophenyl-3-cyanopyridines, **10-13**, and 4-aryl-6-(4-phthalimidophenyl-3-cyanopyridin-2-ones, **14-17** respectively**; (Scheme 1)**.

The structures of 6-(4-phthalimidophenyl) series, **10-17** products were confirmed by spectral data and elemental analysis. Consequently, IR of compound **15,** for instance, exhibited absorption bands at 3320, 2218 cm^{-1} due to NH and CN, respectively, and 1718, 1689 and 1663 cm^{-1} representing three carbonyl groups. Also, ^1H NMR spectrum displayed a singlet signal at δ 3.88 ppm for methoxy protons and two doublets at δ 7.04 and 7.15 ppm for 4Hs of Ar` with *J* constant equal 8.4 *Hz* and another two doublets resonating at δ 7.63 and 8.10 ppm due to 4 Hs of 6-phenyl with *J* constant equal 8.4 *Hz*. Mass spectrum for **15** ($C_{27}H_{17}N_3O_4$**)** showed a molecular ion peak (M^+) at m/z 447.12.

2.2. Biological results and discussion

2.2.1. Antiproliferative screening

All newly 6-(4-benzamido-/4-phthalimido)-3-cyanopyridine derivatives **3-8** and **10-17** were examined for their antiproliferative activities against three cancer cell lines: human prostate carcinoma PC3, human hepatocellular carcinoma HepG2 and breast adenocarcinoma MCF-7 cell lines, using MTT assay. 5-FU was used as a reference drug in this assay.

The most potent cyanopyridines **6-8** and **12, 13** were more active than 5-FU, and the rest of compounds are good to moderately active cytotoxic agents. Besides, SAR analysis elucidated that, when comparing the cytotoxicity of cyanopyridines having flexible 6-benzamidophenyl side chain such as 2-amino analogs **3-5** with their counterparts having 2-hydroxy group, **6-8**; it was clear that 2-OH substituent has a good impact on cytotoxicity of these compounds. However, compounds **12, 13** bearing rigid side chain (4-phthalimidophenyl) displayed higher cytotoxic effect against all cell lines than their counterparts **16, 17** dues to the substituent effect of 2-NH_2 instead of 2-OH, **(Table 1).**

Table 1: *In vitro* [a] cytotoxic activity (IC_{50}, µM) of the tested compounds

Comp. .No

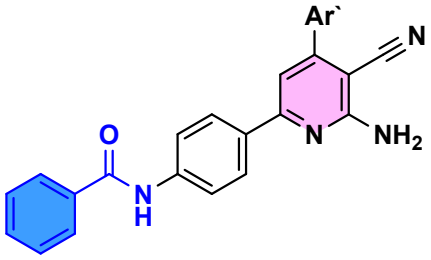

3-5

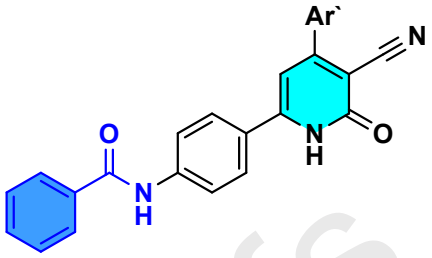

6-8

	Ar´		IC_{50} (µM) ± SE		
			PC 3[b]	HEPG-2[b]	MCF-7[b]
3		CH_3-C_6H_4-4	38.98±2.7	46.53±2.8	62.82±3.2
4	2-OH-C_6H_4		9.7 ±0.85	10.71±0.99	13.39±1.1
5	C_4H_3O		8.18 ± 0.71	10.18±0.75	16.18±0.76
6	4-CH_3-C_6H_4		2.29 ± 0.14	2.96± 0.11	14.02 ± 1.1
7	2-OH-C_6H_4		3.8 ± 0.24	5.84 ± 0.42	8.94±0.77
8	C_4H_3O		5.51 ± 0.46	6.64 ± 0.53	9.18±0.82

Comp. .No

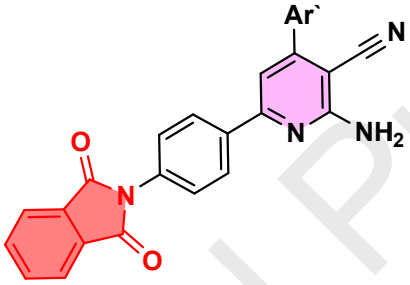

10-13

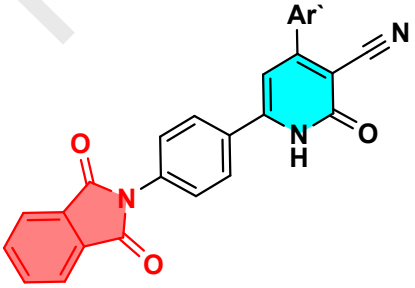

14-17

	Ar´		IC_{50} (µM) ± SE		
			PC 3[b]	HEPG-2[b]	MCF-7[b]
10	4-CH_3-C_6H_4		9.06±0.97	11.41±0.97	13.37±0.97
11	2-OH-C_6H_4		23.56±2.1	35.04±2.4	45.24±2.4
12	4-CH_3O-C_6H_4		5.43±0.51	10.31±0.98	11.22±0.97
13		C_4H_3O	4.82±0.36	5.19±0.43	8.17±0.83
14		CH_3-C_6H_4-4	7.30±0.66	11.16±0.92	14.38±0.85
15		OH-C_6H_4-2	13.26±1.2	15.39±1.1	20.44±1.3
16		CH_3O-C_6H_4-4	17.73±1.5	21.71±2.01	33.76±2.1
17		C_4H_3O	24.57±1.91	31.25±1.6	39.31±2.2
FU- 5			7.53 ±0.57	8.15 ±0.61	7.76 ±0.46

[a] Data represent the mean values of three independent determinations

[b] Cell lines include human prostate carcinoma (PC 3), hepatocellular carcinoma (HEPG-2) and breast adenocarcinoma (MCF-7).

2.2.2. In vitro cytotoxicity screening against normal cell line WI-38

In order to evaluate the safety of the most active compounds **6**, **7**, **8**, **12** and **13** against the normal cell, they were tested for cytotoxicity against normal human diploid lung fibroblast cell line WI-38 to investigate the toxicity and selectivity of these active hits. The selectivity index was calculated using the formula SI= (IC_{50} of WI-38) / (IC_{50} of cancer cell line) **(Table 2)**, which is the measure of the selectivity of the drug candidate towards cancer cells rather than normal cells. When the SI is ≥3, the drug is highly selective. [24] Interestingly, they possessed a remarkable non cytotoxic effect on this normal cell as the concentrations needed to inhibit the viability of WI-38 cells (145.23 - 161.25 µM) is much higher than that needed to inhibit the viability of the various cancer cell lines (2.29 - 14.02 µM). Hence, compounds **6**, **7**, **8**, **12** and **13** were found to be promising anticancer agents especially against prostate cancer (PC 3) with SI values 63.41, 39.07, 27.12, 27.62 and 33.45, respectively. Moreover, compounds **6**, **7**, **8**, **12** and **13** were selective against liver cancer cell line (HEPG-2) with SI range (14.54 – 49.06).

Table 2: cytotoxicity data (IC_{50}, µM) and selectivity index (SI) of **6**, **7**, **8**, **12** and **13**

Parameter	**Compd. No.**				
	6	**7**	**8**	**12**	**13**
IC_{50} (WI-38)	145.23± 0.48	148.45± 0.47	149.44± 0.48	149.95± 0.61	161.25± 0.45
SI (PC 3)	63.41	39.07	27.12	27.62	33.45
SI (HEPG-2)	49.06	25.42	22.51	14.54	31.07
SI (MCF-7)	10.36	16.61	16.28	13.36	19.74

2.2.3. PIM-1 kinase inhibitory activity

The most active cyanopyridine analogs **6-8, 12 and 13** were evaluated for PIM-1 kinase inhibitory activity, to discover novel PIM-1 kinase inhibitors. The percentage of PIM-1 kinase inhibition by our hits was at the range of 76.43-53.33%. Compounds **12, 13** bearing rigid side chains (4-phthalimidophenyl) were higher in PIM-1 kinase inhibitory activity than other analogs, **6-8** having flexible 6-benzamidophenyl side chain. It worth mentioning that, both **12, 13** displayed PIM-1 inhibitory activities in sub-micromolar range (IC_{50} 0.76, 0.63 µM) respectively, **(Table 3, Fig. 1).** PIM-1 inhibition percent of **12, 13** were 73.64 and 76.43% respectively showing higher potencies than that of the reference standard colchicine (64.15%). From enzyme inhibition results, it was clear that compounds **12** and **13** showed potent inhibition of PIM-1.

Table 3: PIM-1 percentage inhibition and IC_{50} values of **6-8**, **12** and **13**

Comp. No.	PIM-1 Inhibition % (Con.10µM)	PIM-1 IC_{50} (µM)
6	53.33	7.04±0.37
7	60.07	2.83±0.14
8	51.98	8.09±0.46
12	73.64	0.76±0.03
13	76.43	0.63±0.02
Colchicine	64.15	3.98±0.15
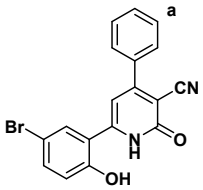	-	0.05

[a] was declared as a potent PIM-1 kinase inhibitor. [25]

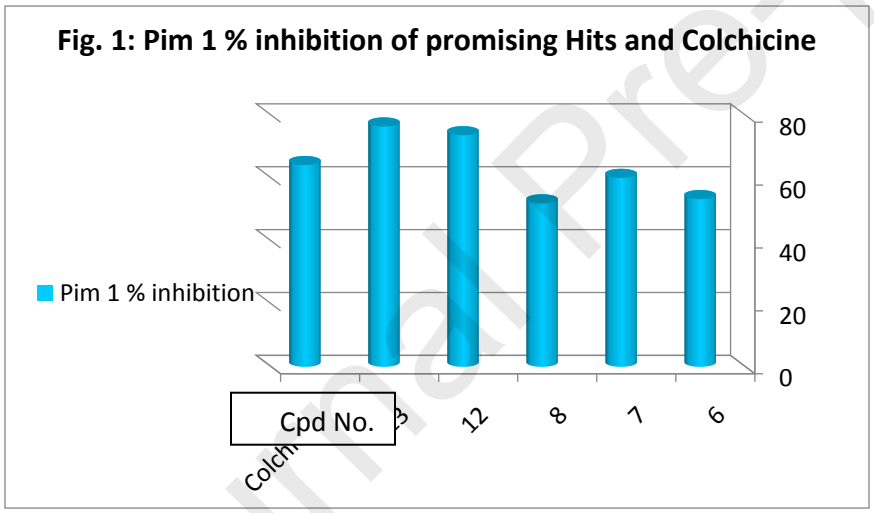

2.2.4. Cell cycle analysis

Appropriate investigating to the potential mechanistic pathways responsible for cell proliferation inhibition by **6- 8, 12** and **13**, cell cycle analysis was tested in the most sensitive cancer cell line, PC 3. As shown in **Table 4** and **Fig. 2**, compounds **6- 8, 12** and **13** increased the cell proportion of G2/M phase and Pre-G1phase, while the cell proportions in G1 and S phases were markedly reduced.

Table 4: Percentages of the PC 3 cell cycle phases of **6- 8**, **12**, **13**, **DMSO** and **5-FU**.

Comp. No.	Conc. (µM)	G0-G1%	S%	G2/M%	Pre-G1%
DMSO / PC-3 (negative control)	0	54.77	36.41	8.82	1.76
FU / PC-3-5 (positive control)	7.53	29.88	27.96	42.16	15.22
6	0.93	21.39	27.41	51.2	27.03
7	1.55	33.92	23.89	42.19	19.26
8	2.1	26.52	25.41	48.07	22.81
12	2.35	37.26	27.22	35.52	13.75
13	1.96	33.72	34.29	31.99	19.64

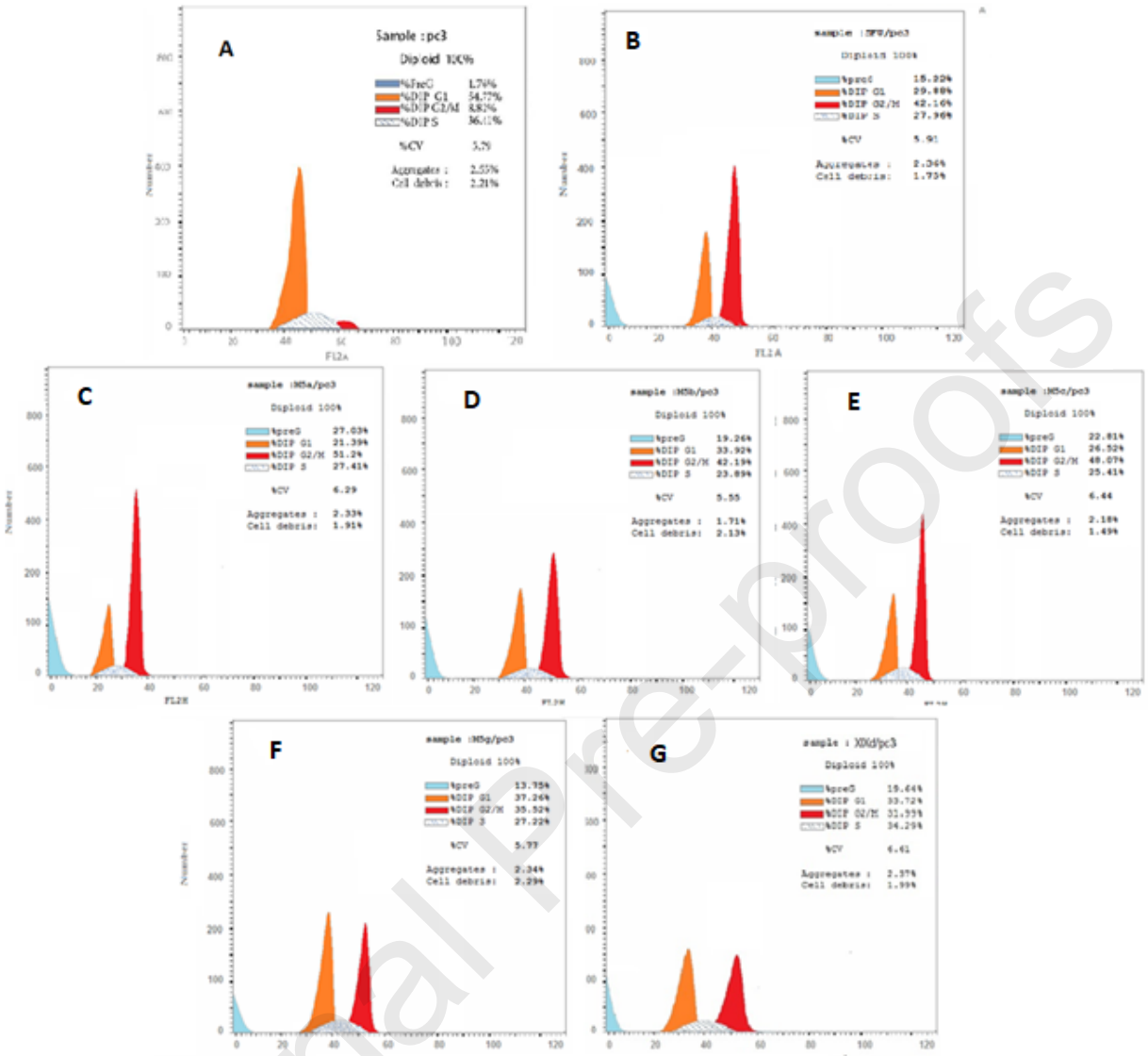

Fig. 2: Cell cycle analysis of PC 3 cells treated with compounds: **DMSO (A)**, **5-FU (B)**, **6 (C)**, **7 (D)**, **8 (E), 12 (F)** and **13 (G)**

2.2.5. Annexin V-FITC apoptosis assay

To confirm whether the Pre-G1phase cells induced by **6-8, 12** and **13** were due to apoptosis or necrosis, these treated compounds with PC 3 cells were further investigated with PI and FITC-Annexin V staining for apoptosis identification. Results declared that all the tested compounds induced apoptosis dependent death. Compounds **7**, **8** and **13** exhibited the highest significant potential for induction of apoptosis (>90), while **6** and **12** displayed 89.6% and 89.3% respectively when compared with 5-FU (85.8%), **(Table 5, Fig. 3).**

Table 5: Percentages of the apoptotic PC 3cells populations in of **6**, **7**, **8**, **12**, **13**, **DMSO** and **5-FU**

Comp. No.	**% Apoptosis**			**Necrosis**
	Total	Early	Late	
DMSO / PC-3 (negative control)	1.76	0.82	0.43	0.51
FU / PC-3-5 (positive control)	15.22	4.94	8.12	2.16
6	27.03	4.82	19.4	2.81
7	19.26	8.29	9.3	1.67
8	22.81	12.14	8.56	2.11
12	13.75	5.19	7.09	1.47
13	19.64	5.88	12.05	1.71

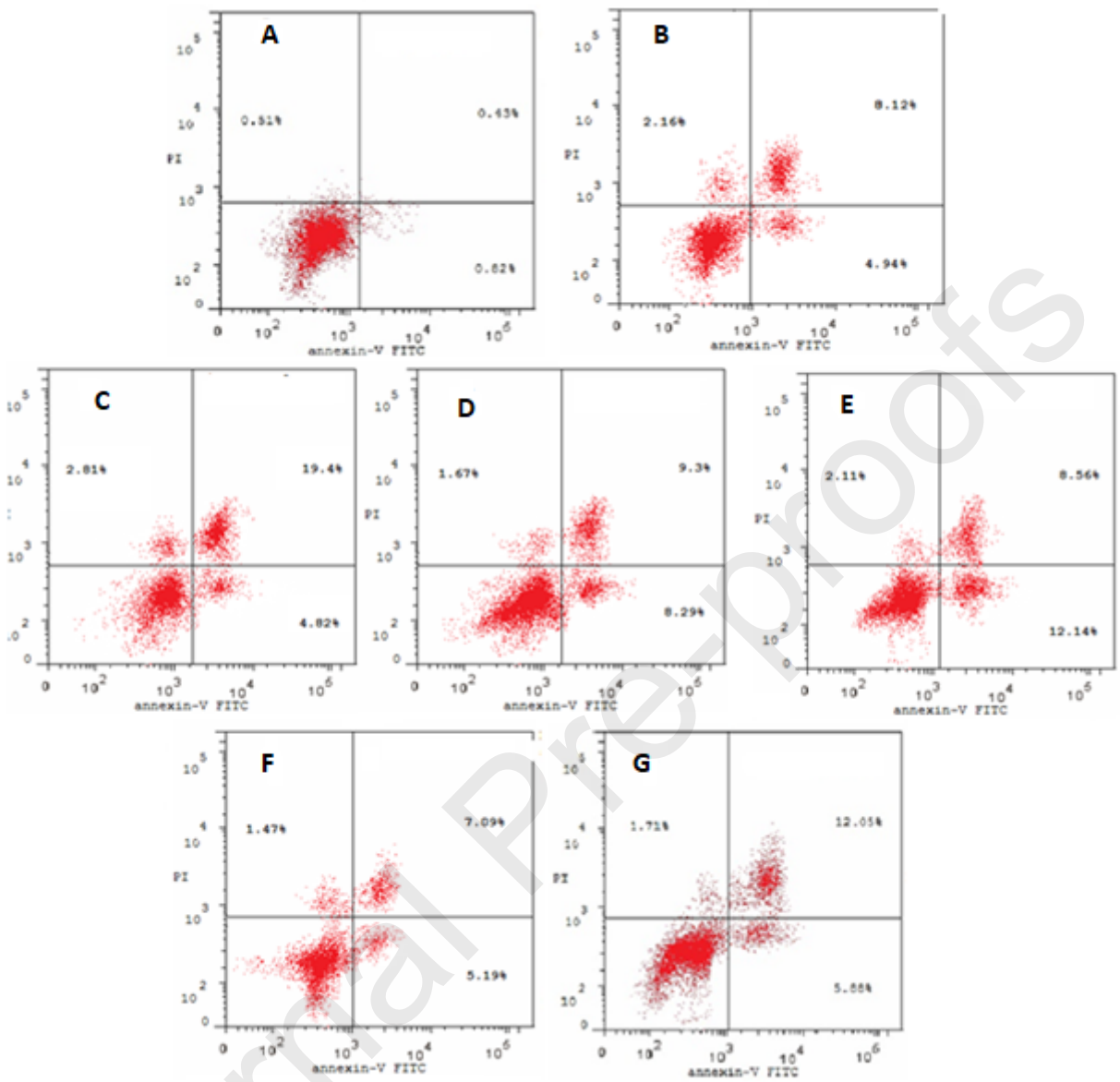

Fig. 3: Histograms display the percentage of PC 3 cell apoptosis distribution of compounds **DMSO (A)**, **5-FU (B)**, **6 (C)**, **7 (D)**, **8 (E), 12 (F) and 13 (G)**

2.2.6. Apoptosis studies

2.2.6.1. *Effects on the level of active caspase 3*

Activation of the caspases' pathway which consider as a hallmark of apoptosis and can be used in cellular assays to quantify activators and inhibitors of the "death cascade." Among caspases, caspase 3 is the vital player that cleaves multiple proteins in the cells, leading to apoptotic cell death. [26] Cyanopyridine analogs **6- 8, 12** and **13** were evaluated for their effect on caspase 3, which is considered as a marker for apoptosis. They showed an increase in the level of

active caspase 3 at the range of 266.0-371.9 Pg/ml compared to that of control (55.3 Pg/ml), **(Table 6).**

Table 6: Caspase 3, BAX and Bcl-2 assays results of **6**, **7**, **8**, **12** and **13**

Comp. No.	Caspase 3 Pg/ml	BAX Pg/ml	Bcl-2 Pg/ml	BAX/Bcl-2 ratio
6	305.7	193.2	1.657	6..116
7	266.0	154.7	2.502	61.83
8	319.4	141.90	2.648	53.59
12	371.9	230.6	1.151	200.35
13	352.9	192.9	1.668	115.65
Control	55.3	18.14	5.418	3.35

2.2.6.2. *Effects on mitochondrial apoptosis pathway proteins Bax and Bcl-2*

The B-cell lymphoma protein 2 (Bcl-2) families plays a crucial role in tumor progression or inhibition of the intrinsic apoptotic pathway triggered by mitochondrial dysfunction, with Bcl-2 itself and BAX as pro-apoptotic proteins. [27] Several direct BAX activators have been identified to hold promise for cancer therapy with the advantages of specificity and the potential of overcoming chemo- and radioresistance. It is possible that Bcl-2 levels in the mitochondrial membrane must decrease if BAX levels in the mitochondria are to rise. The effect of the most active cyanopyridine analogs **6- 8, 12** and **13** on the expression levels of BAX and Bcl-2 were determined**.** Analyzing the results disclose that all the tested derivatives caused upregulation in the level of the proapoptotic protein; BAX while it markedly downregulated the levels of the antiapoptotic proteins Bcl-2, **(c.f. Table 6).** As of literature study, there is a strong indication that the ratio of pro-apoptotic BAX versus antiapoptotic Bcl-2 proteins indicates the susceptibility of cancer cells to undergo apoptosis more accurately. [28] Consistent with our results, compound **12** increased the BAX/Bcl-2 ratio by approximately 60 folds, as well as compounds **6** and **13** boosted the BAX/Bcl-2 ratio by almost 35 folds, while **7** and **8** enhanced the ratio by around 16 and 18 folds, respectively, as compared to the control. These findings support the effectiveness as apoptosis induction effect of compounds **6- 8, 12** and **13**.

2.3. Molecular modeling and *in silico* predictions

2.3.1. *Molecular docking study of ligand with PIM-1*

Molecular docking was performed to understand the binding and interactions of derivative **13** inside the known crystal structure of PIM-1 kinase protein (PDB ID: 2OBJ), [25] using the Molecular Operating Environment (MOE 2010) software. VRV was initially re-docked into the active site of PIM-1 **(Fig. 4)** to validate docking procedures. The result revealed superimposition of the redocked ligand above native VRV with RMSD of 0.88 Å.

Analysis of docking results of compound **13** showed that it had comparable docking score energy with that of the reference ligand (VRV). Also, its binding mode to PIM-1 protein was like

that of the VRV in that it occupied the ATP-binding pocket, showing hydrogen bonding interaction with the hinge region residue (**Fig. 5**). As we know, Lys67 is critical to PIM-1 catalytic activity and in ATP-bound structure, where the nitrogen of CN group acts as hydrogen bond acceptor to the highly conserved residue, Lys67, in addition to arene-H interaction of the pyridine core to Val52. The central phenyl was recognized by Leu44 (NTD), making hydrophobic interaction and binds through arene-H interaction to Leu174 (CTD). Moreover, the phthalimido moiety contributes to PIM-1 affinity via making additional HBA via carbonyl oxygen of phthalimido moiety with Asp128, arene-H bonding to Gln127 and hydrophobic interaction with Val126 (Hinge region) and Asp131**.** The hydrophobic interactions described above determine the affinity of inhibitor for the ATP-binding pocket.

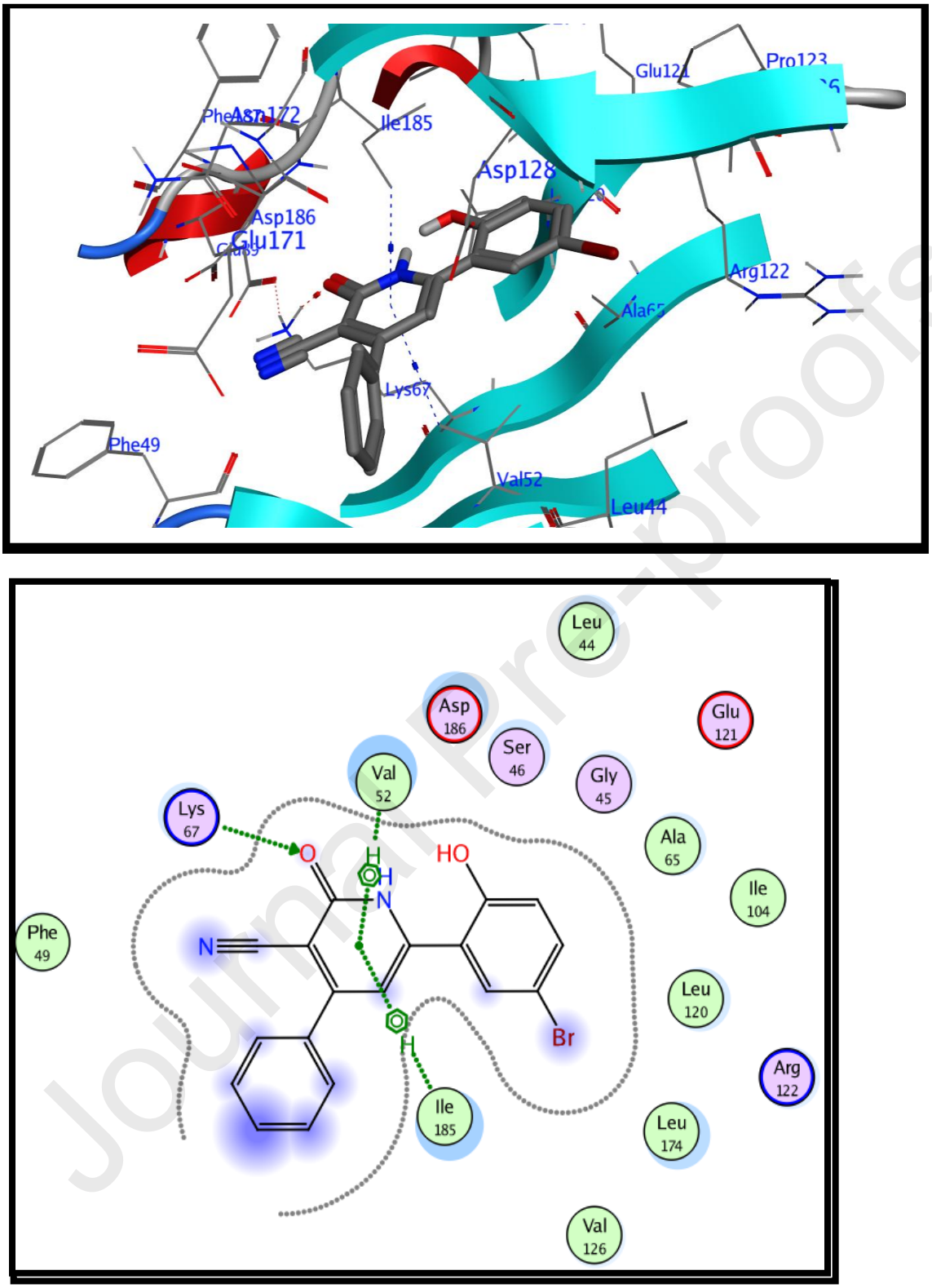

Fig. 4: Docking and binding pattern of the ligand, (VRV), into PIM-1 kinase active site (PDB 2OBJ) in 3D (upper panel) and 2D (lower panel)

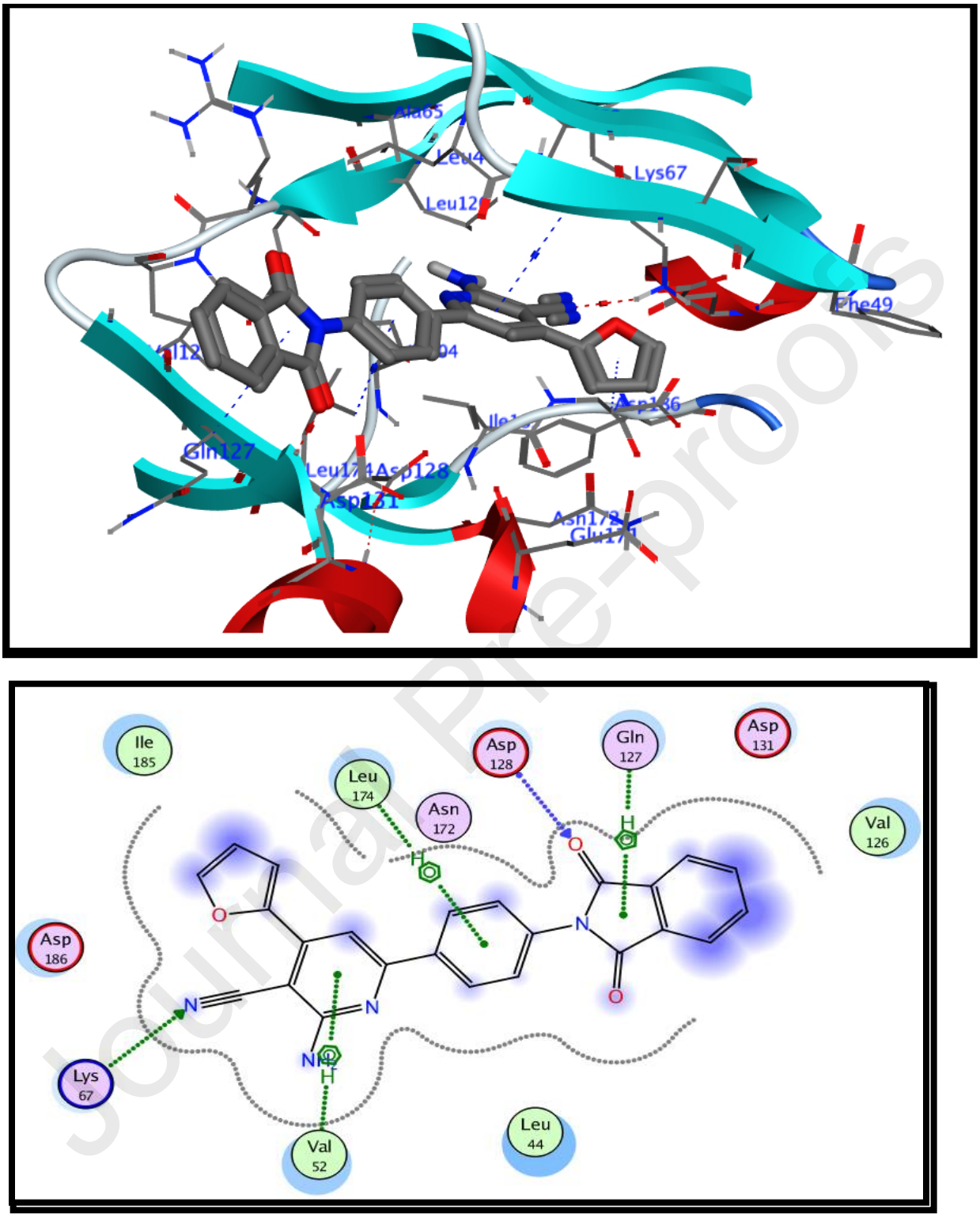

Fig. 5: Docking and binding pattern of compound **13** into PIM-1 kinase active site (PDB 2OBJ) in 3D (upper panel) and 2D (lower panel)

2.3.2. *In silico prediction of physicochemical and ADME properties and pharmacokinetic profile*

In silico ADME data (absorption, distribution, metabolism, and excretion), provide first key insights into how the human body will eventually treat a drug. Poor pharmacokinetic parameters constitute a significant reason for the lack of therapeutic activity of some drug candidates. Consequently, evaluation of the pharmacokinetic parameters of drug candidates at an early stage of screening is a vital step in the drug development process that can directly lead optimization efforts into improved hits [29] and reduce the late-stage attrition in drug discovery programmes. Lipinski has emerged in a set of rules focusing attention on the importance of lipophilicity (octanol-water partition or LogP), the number of hydrogen bond acceptors (HBA) and donors (HBD), and molecular weight (MW). These rules considered as basic assistance to relate physicochemical properties with effective drug development by examination of the structures of orally administered drugs, and drug candidates. An orally available drug candidate is compatible with Lipinski's rule if LogP is no more than 5, MW is less than 500, number of HBD is less than 5 and number of HBA is less than 10. [30] Additionally, Veber [31] rule defines drug-likeness constraints as rotatable bond count ≤ 10; as the more flexible the molecule, the less likely it is to be orally active, while polar surface area (TPSA) could be used as a factor instead of the number of hydrogen bonding groups. TPSA of less than 140 Å2 should present high oral bioavailability in rats.

In this, Molinspiration, [32] Molsoft, [33] Pre-ADMET, [34] Data warrior, [35] PAINS-Remover, [36] and SwissADME, [37] software were used to evaluate the pharmacokinetic parameters of the most active compounds **6**, **7**, **8**, **12** and **13**. It was found that the physicochemical properties (Table7) of all the active compounds have Lipinski zero violation except for one compound **6** which has only one violation LogP value 5.02 (>5), but it still stays in the orally bioavailable compounds. Furthermore, they all showed NROTB values of 3 and 4(<10), and TPSA values range of 85.75 and 120.01 Å2 (<140 Å2). Additionally, absorption (% ABS) was estimated by using the equation % ABS = 109 – (0.345 x TPSA), [38] founding that the calculated % ABS of all these hits ranged between 67.60% and 79.42%, demonstrating that these synthesized derivatives may have the required cell membrane permeability and bioavailability. All compounds have rotatable bonds between 3 and 4 which indicating molecular flexibility to their bio target.

Alternatively, Molsoft software was used to evaluate the solubility and drug-likeness model score for the active derivatives. Aqueous solubility is a well-known parameter that, affect absorption and distribution qualities significantly. **6**, **7**, **8**, **12** and **13** achieved the requirements of solubility with values hits ranged between of 8.38 and 62.71 mg/L (more than 0.0001 mg/L). Compounds showing positive drug-likeness model scores are recognized as drug-like and can behave as drug molecules. A positive model-score was predicted for compound **7** and **8** (0.49 and 0.04, respectively) while that for compound **6**, **12** and **13** was negative (-0.14, -0.21 and -0.51, respectively), as well as 5-FU (-1.07). Likewise, *in silico* assessment of the following

pharmacokinetic parameters was performed using Pre-ADMET software: Caco2 (human colon adenocarcinoma) permeability coefficient, Human intestinal absorption (HIA), Brain-blood barrier partition coefficient (BBB) and human plasma protein binding (PPB) (Table 7). **6**, **7**, **8**, **12** and **13** showed medium cell permeability in the Caco- 2 cell model with values between 21.01 and 21.52 nm/s. They showed high human intestinal absorption values (93.7107 - 98.3290 %) indicating very well-absorbed compounds, which is better than that of 5-FU (75.9253 %). Furthermore, they demonstrated low BBB penetration capability (0.0251 - 0.0886). All the biologically active derivatives were found to be highly bound to human plasma proteins (92.7812 - 95.3666 %).

Toxicity risk assessment tries to locate substructures within the chemical structure being indicative of a toxicity risk within one of four major toxicity classes (Mutagenicity, Tumorigenicity, Irritant, and Reproductive Effective). The overall toxicities of the most active synthesized compounds and compared them with three standard anticancer agents, that is, 5-FU, Colchicine and Sorafenib, were determined using the Datawarrior software. Datawarrior predicted that derivatives **6** and **7** had tumorigenic toxicity. While **8** was predicted to have high mutagenic and tumorigenic effect. On the other hand, **12** and **13** were found to pass the toxicity risk assessment. Conversely, 5-FU was predicted to have high mutagenic, tumorigenic, irritant and reproductive toxicities, whereas colchicine was predicted to have a high reproductive effect.

Another important consideration during preclinical analysis trial was to analyse the P-glycoprotein (P-gp) non-substrate candidature. P-gp works as efflux transporter which pumps drugs and other compounds and its substrate out of the cell, which was found to be one of explanation for its resistance to various chemotherapeutics for cancer. It has been found that P-gp is a critical transporter of drug which consequently results in resistance to anticancer drugs like Imatinib, Lonafarnib, and Taxanes. [39] Therefore, the hits had been analyzed using the SwissADME website. We found that all the synthesized compounds are not substrates of P-gp protein (**Table 7**), indicating that these hits have very less chance to efflux out of the cell, thus resulting in a maximum effect. Bioavailability is an index of the amount of drug present in the plasma and is considered as the most crucial factor affecting absorption. Interestingly, all the synthesized derivatives were found to have high bioavailability scores equal to that of 5-FU.

SwissADME Synthetic Accessibility (SA) Score is based primarily on the assumption that the frequency of molecular fragments in 'really' obtainable molecules correlates with the ease of synthesis, the score is normalized to range from 1 (very easy) to 10 (very difficult to synthesize) . [37] SA scores of all the analogs were found to be between 2.99 and 3.22, indicating that they can be readily synthesized on a large scale.

Pan-assay interference compounds (PAINS) are chemical compounds that often give false positive results in high-throughput screens. [40] PAINS tend to react non-specifically with numerous biological targets rather than specifically affecting one desired target . [41] So, it is

essential to check any PAINS alert of the newly synthesized derivatives. PAINS was performed by SwissADME, [[37]] and PAINS-Remover [36] displayed zero alerts to all the hits.

Collectively and based on the estimated ligand efficiency, drug likeness and pharmacokinetic predictors, these active compounds considered as a pharmacologically active framework that should be considered on progressing further potential hits.

Table 7: *In silico* physicochemical properties, ADME and ligand efficiency data of compounds **6-8**, **12** and **13**

							Compd no
Property	**6**	**7**	**8**	**12**	**13**	**FU-5**	**Colchicine**
Molinspiration							
logP[a]	5.02	4.31	3.71	4.44	3.85	0.59-	1.10
MW[b]	405.46	407.43	381.39	432.44	406.40	130.08	399.44
HBA[c]	5	6	4	6	5	7	1
HBD[d]	2	3	2	2	1	3	7
Lipinski's violation	1	0	0	0	0	0	0
TPSA[e]	85.75	105.98	98.89	120.01	114.92	65.72	83.11
ABS[f]%	79.42	72.44	74.88	67.60	69.35	86.33	80.33
NROTB[g]	4	4	4	3	3	0	5
Molsoft							
S (mg/L) [h]	8.38	41.80	62.71	55.64	62.51	5809.82	6013.76
Drug likeness model score	0.14-	0.49	0.04	0.21-	0.51-	1.07-	0.90
Pre-ADME							
Caco2[I]	21.49	21.01	21.52	21.01	21.15	17.25	37.47
HIA[J]	95.77	93.7107	95.4748	96.2023	98.3290	75.9253	96.8889
BBB[K]	0.0335	0.0375	0.0251	0.0346	0.0886	0.1995	0.0127
PPB[l]	95.3666	94.4651	92.7812	94.7186	92.8878	8.3130	39.3768
Datawarrior							
Mutagenicity[m]	None	None	High	None	None	High	None
Tumorigenicity[m]	High	High	High	None	None	High	None
Irritant[m]	None	None	None	None	None	High	None
Reproductive effective[m]	None	None	None	None	None	High	High
SWISS ADME							
Pgp substrate	No	No	No	No	No	No	Yes
Bioavailability Score	0.55	0.55	0.55	0.55	0.55	0.55	0.55
Synthetic Accessibility	3.01	2.99	3.17	3.05	3.22	1.52	3.87
PAINS-Remove[n]							
Pains alert	0	0	0	0	0	0	0

[a] LogP: logarithm of compound partition coefficient between n-octanol and water.
[b] MW: molecular weight.
[c] HBA: number of hydrogen bond acceptors.
[d] HBD: number of hydrogen bond donors.
[e] TPSA: topological polar surface area.
[f] %ABS: percentage of absorption.
[g] NROTB: number of rotatable bonds.

[h] S: aqueous solubility.
[i] Caco2: permeability through cells derived from human colon adenocarcinoma; Caco2 values < 4 nm/s (low permeability), values ranged from 4 to 70 nm/s (medium permeability) and values > 70 nm/s (high permeability).
[J] HIA: percentage human intestinal absorption; HIA values ranged from 0 to 20% (poorly absorbed), values ranged from 20 to 70% (moderately absorbed) and ranged from 70 to 100% (well absorbed).
[K]BBB: blood-brain barrier penetration; BBB values < 0.1 (low CNS absorption), values ranged from 0.1 to 2 (medium CNS absorption) and values > 2 (high CNS absorption).
[l] PPB: plasma protein binding; PPB values < 90% (poorly bound) and values > 90% (strongly bound).
[m] Toxicity Risk Assessment.
[n] PAINS Alerts were performed by SwissADME and PAINS-Remover.

3. Conclusion

All the examined cyanopyridine hits are potent to moderate cytotoxic on the three cancer cell lines, prostate carcinoma PC3, human hepatocellular carcinoma HepG2 and breast adenocarcinoma MCF-7 compared to the reference standard 5-FU. For PIM-1 inhibition, compounds bearing 6-phthalimidophenyl is more favored than those with 6-benzamidophenyl side chain. The most potent compounds were further selected to investigate its apoptotic inducing effect. They showed an increase in the level of active caspase 3 by 7-folds, an upregulation in BAX and downregulation in Bcl-2 levels, compared to the control cells. These compounds cause cell cycle arrest at G2/M and induce apoptosis via enhancement of Pre-G in cell cycle analysis. Finally, molecular modeling studies were carried out on compound **13**, showed perfect fitting in PIM-1 active site. Furthermore, drug-likeness assessment via Molinspiration, Molsoft, Pre-ADMET, Data warrior, SWISS ADME and PAINS-remover software and websites elucidated their full compliance with Lipinski's rule, favorable physicochemical properties, and convenient predicted pharmacokinetic parameters. These results have improved the understanding of the molecular mechanism of tumor genesis of prostate cancer to provide novel insights for the treatment of prostate cancer.

4. Experimental section

4.1. Chemistry

Reagents and solvents were purchased from usual commercial suppliers and were used without further purification. Yields reported refer to purified products. All reactions were routinely checked by thin-layer chromatography (TLC) on Merck Silica Gel 60 F_{254} (0.25mm thick) and visualization was performed with UV lamp. Melting points were measured in open capillary tubes using Stuart SMP3 apparatus. IR spectra (KBr) were measured on a Shimadzu FT/IR 1650 (Perkin Elmer) spectrometer. ^{1}H and ^{13}C NMR spectra were recorded on a Brüker Advance-400 instrument (400 MHz for ^{1}H and 100 MHz for ^{13}C) in DMSO-d6 Chemical shifts (δ) are reported in ppm relative to TMS as an internal standard, or to the solvent in which the spectrum was recorded. Mass spectra were performed on a Shimadzu GS/MS-QP 2010 plus spectrometer at 70 eV.

4.1.1. *N-(4-acetylphenyl)benzamide (**2**)*

To a solution of p-aminoacetophenone (1.35g, 0.01mol) in dimethyl formamide (20 ml) an equimolar amount of benzoyl chloride (1.40g, 0.01mol) was added. The mixture was stirred at 0 ℃ for 3 h, after which crushed ice was added with continuous stirring. A heavy precipitate was obtained, which was filtered, washed with water and after drying it was crystallized out from ethanol. The yield was 95 % and the melting temperature was 200-202℃. [19]

4.1.2. *General procedure for the synthesis of N-(4-(6-Amino-5-cyano-4-arylpyridin-2-yl)phenyl) benzamides **(3-5)***

A mixture of **2** (2.39g, 0.01 mol), different aryl aldehydes (0.01 mol), ammonium acetate (6.16g, 0.08 mol) and malononitrile (0.66 g, 0.01 mol) were refluxed in ethanol (20 ml) for 6-12 h. After completion of reaction, it was further cooled and filter the solid. The solid was purified by ethanol with 85 - 95% yields.

*4.1.2.1. N-(4-(6-Amino-5-cyano-4-(p-tolyl)pyridin-2-yl)phenyl) benzamide(**3**).* **Yield** 88 %; **m.p.** 100-102 ^{o}C; **IR** (KBr, cm^{-1}): 3345, 3300 (NH, NH_2) , 2198 (C≡N), 1650 (C=O), 1587 (C=N); **^{1}H NMR** (DMSO-d_6) δ (ppm): 2.38 (s, 3H, CH_3), 7.10 (s, H, pyridine- H), 7.36 (d, 2H, $H_{3,5}$ Ar`-H), 7.51 - 7.60 (m, 4H, $H_{2,6}$ Ar`-H, $H_{3,5}$Phenyl-H), 7.77 -7.79 (t, H, H_4 phenyl-H), 7.92 – 8.01 (m, 4H, $H_{2,6}$ Ar-H, $H_{2,6}$ Phenyl-H), 8.18 (d, 2H, $H_{3,5}$ Ar-H), , 10.42, 10.51 (2s, 3H, NH, NH_2; exchangeable with D_2O); **^{13}C NMR** (DMSO-d_6) δ (ppm): 21.46, 90.12, 114.17, 115.52, 119.91, 127.53, 128.08, 128.24, 128.92, 129.68, 132.08, 132.27, 133.85, 135.20, 154.87, 158.58, 164.13, 166.40; **MS**, m/z: 404 (M^+, 100 %), 405 [$(M+1)^+$, 31.4 %], 406 [$(M+2)^+$, 5.25 %]; Anal. Calcd. For $C_{26}H_{20}N_4O$ (404.16): C, 77.21; H, 4.98; N, 13.85, Found: C, 77.43; H, 5.12; N, 14.08.

*4.1.2.2.N-(4-(6-amino-5-cyano-4-(2-hydroxyphenyl)pyridin-2-yl)phenyl) benzamide (**4**).* **Yield** 85 %; **m.p.** 140 -142 ^{o}C; **IR** (KBr, cm^{-1}): 3429, 3321, 3240 (OH, NH, NH_2) , 2195 (C≡N), 1656 (C=O), 1603 (C=N), 1562 (C=C); **^{1}H NMR** (DMSO-d_6) δ (ppm): 6.89 -7.00 (m, 2 H, $H_{3,5}$ Ar`-H), 7.14 (s, H, pyridine- H), 7.28 - 7.31 (t, H, $H_4$ Ar`-H), 7.62 - 7.75 (m, 4H, H_6 Ar`-H, $H_{3,4,5}$ Phenyl-H), 7.91- 8.03 (m, 4H, $H_{2,6}$ Ar-H , $H_{2,6}$ phenyl-H), 8.39 (d, H, $H_{3,5}$ Ar-H), 10.45, 10.53, 12.19 (3s, 4H, NH, NH_2, OH; exchangeable with D_2O); **^{13}C NMR** (DMSO-d_6) δ (ppm): 90.89, 111.44, 115.63, 117.99, 119.37, 122.89, 128.27, 128.92, 129.96, 131.28, 133.97, 134.87, 136.52, 154.55, 158.59, 161.35, 164.30; **MS**, m/z: 406 (M^+, 1.02 %), 407 [$(M+1)^+$, 8.03 %], 408 [$(M+2)^+$, 3.54 %]; Anal. Calcd. For $C_{25}H_{18}N_4O_2$ (406.14): C, 73.88; H, 4.46; N, 13.78, Found: C, 74.19; H, 4.57; N, 14.01.

*4.1.2.3.N-(4-(6-amino-5-cyano-4-(furan-2-yl)pyridin-2-yl)phenyl)benzamide (**5**).* **Yield** 95 %; **m.p.** 304-306 ^{o}C; **IR** (KBr, cm^{-1}): 3440 - 3353 (NH, NH_2) , 2204 (C≡N), 1652 (C=O), 1597 (C=N), 1521 (C=C); **^{1}H NMR** (DMSO-d_6) δ (ppm): 6.76 -6.77 (m, 1H, H_4 Ar`-H), 7.08 (d, 1H, $H_5$ Ar`-H), 7.14 (s, H, pyridine- H), 7.53 -7.62 (m, 3 H, $H_{3,4,5}$ Phenyl-H), 7.89 – 7.99 (m, 3H, H_3 Ar`-H, $H_{2,6}$ Ar-H), 8.08 – 8.14 (m, 4H, $H_{2,6}$ Phenyl-H, $H_{3,5}$ Ar-H), 10.36, 10.44 (2s, 3H, NH, NH_2; exchangeable with D_2O); **^{13}C NMR** (DMSO-d_6) δ (ppm): 89.27, 107.37, 111,49 113.47, 120.11,

120.44, 127.99, 128.20, 128.29, 128.94, 132.89, 134.20, 134.89, 141.67, 151.27, 156.53, 161.63, 166.22; **MS**, m/z: 380 (M^+, 85.37 %), 381 [$(M+1)^+$, 11.53%]; Anal. Calcd. For $C_{23}H_{16}N_4O_2$ (380.13): C, 72.62; H, 4.24; N, 14.73, Found: C, 72.80; H, 4.41; N, 14.97.

4.1.3. *General procedure for the synthesis of N-(4-(5-Cyano-6-oxo-4-(aryl)-1,6-dihydropyridin-2-yl)phenyl)benzamides* ***(6-8)***

A mixture of **2** (2.39g, 0.01 mol), different aryl aldehydes (0.01 mol), ammonium acetate (6.16g, 0.08 mol) and ethyl cyanoacetate (1.13g, 0.01 mol) were refluxed in ethanol (20 ml) for 6-12 h. After completion of reaction, it was further cooled and filter the solid. The solid was purified by ethanol with 80 - 90% yields.

*4.1.3.1. N-(4-(5-Cyano-6-oxo-4-(p-tolyl)-1,6-dihydropyridin-2-yl)phenyl) benzamide (**6**).* **Yield** 80%; **m.p.** 255 - 257 ^oC; **IR** (KBr, cm^{-1}): 3430, 3356 (2 NH) , 2218 (C≡N), 1723, 1674 (2C=O), 1598 (C=C); **^{1}H NMR** (DMSO-d_6) δ (ppm): 2.41 (s, 3H, CH_3-Hs), 7.15 (d, 2H, $H_{3,5}$ Ar`-H, *J* = 8 Hz), 7.41 (d, 2H, $H_{2,6}$ Ar`-H, *J* = 8 Hz), 7.56 – 7.63 (m, 5H, $H_{2,6}$ Ar-H, $H_{3,4,5}$ Phenyl-H), 7.94 – 7.99 (m, 4H, $H_{2,6}$ Phenyl-H, $H_{3,5}$ Ar-H), 8.36 (s, H, pyridine- H) , 10.51, 10.56 (2s, 2H, NH; exchangeable with D_2O); **^{13}C NMR** (DMSO-d_6) δ (ppm): 21.39, 101.62, 116.27, 116.89, 120.43, 128.17, 128.23, 128.27, 128.66, 128.91, 132.35, 132.48, 133.40, 135.04, 136.86, 155.42, 157.08, 159.88, 162.48, 166.54; **MS**, m/z: 405 (M^+, 3.57 %), 406 [$(M+1)^+$, 1.73%], 407 [$(M+2)^+$, 1.47%]; Anal. Calcd. For $C_{26}H_{19}N_3O_2$ (405.15): C, 77.02; H, 4.72; N, 10.36, Found: C, 76.89; H, 4.87; N, 10.59.

4.1.3.2.N-(4-(5-Cyano-4-(2-hydroxyphenyl)-6-oxo-1,6-dihydropyridin-2-yl)phenyl) benzamide (7). **Yield** 90%; **m.p.** 321 - 323 ^oC; **IR** (KBr, cm^{-1}): 3474, 3349, 3299 (OH, 2 NH) , 2203 (C≡N), 1706, 1675 (2C=O), 1611 (C=C); **^{1}H NMR** (DMSO-d_6) δ (ppm): 7.33 – 7.46 (m, 4H, Ar`-Hs), 7.51 – 7.72 (m, 5H, , $H_{2,6}$ Ar-H, $H_{3,4,5}$ Phenyl-H,), 7.99 – 8.08 (m, 4H, $H_{3,5}$ Ar-H, $H_{2,6}$ Phenyl-H), 8.33 (H, pyridine-H), 10.48, 10.55, 11.65 (3s, 3H, 2 NH, OH; exchangeable with D_2O); **^{13}C NMR** (DMSO-d_6) δ (ppm): 104.64, 115.55, 116.72, 117.38, 120.38, 121.76, 126.52, 127.06, 128.47, 128.93, 129.55, 130.95, 132.36, 134.08, 135.07, 155.34, 160.50, 161.36, 164.03, 166.41; **MS**, m/z: 407 (M^+, 9.74 %), 408 [$(M+1)^+$, 3.81%]; Anal. Calcd. For $C_{25}H_{17}N_3O_3$ (407.13): C, 73.70; H, 4.21; N, 10.31; Found: C, 73.94; H, 4.37; N, 10.48.

*4.1.3.3.N-(4-(5-Cyano-4-(furan-2-yl)-6-oxo-1,6-dihydropyridin-2-yl)phenyl) benzamide (**8**)* **Yield** 85%; **m.p.** 104 - 106 ^oC; **IR** (KBr, cm^{-1}): 3404, 3353 (2 NH) , 2222 (C≡N), 1717, 1675 (2C=O), 1620 (C=C); **^{1}H NMR** (DMSO-d_6) δ (ppm): 6.84 (d, H, H_4 Ar`-H), 7.50 – 7.60 (m, 6H, $H_5$ Ar`-H, $H_{2,6}$ Ar-H, $H_{3,4,5}$ Phenyl-H), 7.93 – 7.96 (m, 4H, $H_{3,5}$ Ar-H, $H_{2,6}$ Phenyl-H), 8.12 (s, H, pyridine-H), 8.20 (d, H, H_3 Ar`-H), 10.52, 10.53 (2s, 2H, 2NH; exchangeable with D_2O); **^{13}C NMR** (DMSO-d_6) δ (ppm): 104.38, 110.05, 114.80, 115.75, 119.90, 120.03, 125.14, 126.11, 126.99, 128.27, 128.92, 132.36, 135.04, 139.60, 144.08, 150.58, 159.05, 160.53, 162.68, 166.46; **MS**,

m/z: 381 (M^+, 8.62 %); Anal. Calcd. For $C_{23}H_{15}N_3O_3$ (381.11): C, 72.43; H, 3.96; N, 11.02; Found: C, 72.70; H, 4.11; N, 11.34.

4.1.4. *2-(4-acetylphenyl)isoindoline-1,3-dione (**9**)*

Phthalic anhydride (1.48 g, 0.01 mole) and p-aminoacetophenone (1.35g, 0.01 mol) were refluxed in (50 ml) acetic acid for 4 hour. The reaction mixture was filtered off while hot and the solvent was evaporated. The solid separated was filtered and recrystallized from ethanol. The yield was 90 % and the melting temperature was 248-250℃. [42]

4.1.5. *General procedure for the synthesis of 2-Amino-6-(4-(1,3-dioxoisoindolin-2-yl)phenyl)-4-(aryl)nicotinonitriles **(10-13)***

A mixture of **9** (2.65g, 0.01 mol), different aryl aldehydes (0.01 mol), ammonium acetate (6.16g, 0.08 mol) and and malononitrile (0.66 g, 0.01 mol) were refluxed in glacial acetic acid (15 ml) for 12 h. After completion of reaction, it was further cooled and filter the solid. The solid was purified by ethanol with 70 - 89% yields.

*4.1.5.1.2-Amino-6-(4-(1,3-dioxoisoindolin-2-yl)phenyl)-4-(p-tolyl) nicotinonitrile (**10**)*. **Yield** 84%; **m.p.** 189 - 191 ^oC; **IR** (KBr, cm^{-1}): 3390, 3330 (NH_2) , 2206 (C≡N), 1717, 1679 (2C=O), 1658 (C=N), 1599 (C=C); **^{1}H NMR** (DMSO-d_6) δ (ppm): 2.39 (s, 3H, CH_3-Hs), 5.58 (s, 2H, NH_2; exchangeable with D_2O), 7.27– 7.39 (m, 4H, Ar`-Hs), 7.63 (d, 2H, $H_{2,6}$ Ar-H, J = 8.4 Hz), 7.83 (s, H, pyridine-H), 7.86 – 8.01 (m, 4H, Phthalimide-Hs), 8.10 (d, 2H, $H_{3,5}$ Ar-H, J = 8.4 Hz); **^{13}C NMR** (DMSO-d_6) δ (ppm): 21.71, 105.65, 114.33, 118.60, 123.40, 124.03, 127.51, 129.24, 129.78, 129.92, 130.32, 130.61, 131.97, 133.07, 134.79, 136.49, 155.26, 156.78, 169.70; **MS**, m/z: 430.34 (M^+, 19.31 %), 431.26 [$(M+1)^+$, 11.43%], 432.00 [$(M+2)^+$, 2.67%]; Anal. Calcd. For $C_{27}H_{18}N_4O_2$ (430.17): C, 75.34; H, 4.21; N, 13.02; Found: C, 75.43; H, 4.15; N, 13.04.

*4.1.5.2.2-Amino-6-(4-(1,3-dioxoisoindolin-2-yl)phenyl)-4-(4-methoxy phenyl) nicotinonitrile (**11**)*. **Yield** 70%; **m.p.** 182 - 184 ^oC; **IR** (KBr, cm^{-1}): 3406, 3347 (NH_2) , 2219 (C≡N), 1719, 1690 (2C=O), 1620 (C=N), 1595 (C=C); **^{1}H NMR** (DMSO-d_6) δ (ppm): 3.74 (s, 3H, CH_3O-Hs), 5.75 (s, 2H, NH_2; exchangeable with D_2O), 7.13 (d, 2H, $H_{3,5}$ Ar`-H), 7.68 – 7.74 (m, 4H, $H_{2,6}$Ar`-H, $H_{2,6}$ Ar-H), 7.83 (s, H, pyridine-H), 7.91 – 8.02 (m, 4H, Phthalimide-Hs), 8.11 (d, 2H, $H_{3,5}$ Ar-H); **^{13}C NMR** (DMSO-d_6) δ (ppm): 55.93, 105.20, 114.97, 115.30, 123.40, 127.76, 128.10, 129.84, 130.54, 132.06, 132.92, 133.08, 134.80, 155.30, 156.59, 162.24, 163.83, 169.71; **MS**, m/z: 446.49 (M^+, 5.53 %), 447.91 [$(M+1)^+$, 1.17%]; Anal. Calcd. For $C_{27}H_{18}N_4O_3$ (446.14): C, 72.64; H, 4.06; N, 12.55; Found: C, 72.89; H, 4.24; N, 12.71.

*4.1.5.3.2-Amino-6-(4-(1,3-dioxoisoindolin-2-yl)phenyl)-4-(2-hydroxyphenyl) nicotinonitrile (**12**)*. **Yield** 89%; **m.p.** 375 - 377 ^oC; **IR** (KBr, cm^{-1}): 3438, 3300 (OH, NH_2) , 2199 (C≡N), 1707, 1669 (2C=O), 1606 (C=N), 1558 (C=C); **^{1}H NMR** (DMSO-d_6) δ (ppm): 5.59 (s, 2H, NH_2; exchangeable with D_2O), 7.31 – 7.37 (m, 3H, $H_{3,4,5}$ Ar`-H), 7.43 (d, $H_{2,6}$ Ar-H, J = 8.4 Hz), 7.60 (

s, H, pyridine-H), 7.85 (d, H, H_6 Ar`-H), 8.00 – 8.19 (m, 4H, Phthalimide-Hs), 8.29 (d, 2H, $H_{3,5}$ Ar-H, *J* = 8.4 Hz), 11.66 (s, H, OH; exchangeable with D_2O); **^{13}C NMR** (DMSO-d_6) δ (ppm): 105.88, 111.05, 116.00, 118.08, 123.96, 124.87, 127.43, 128.99, 129.21, 131.03, 132.02, 133.97, 135.17, 152.50, 157.55, 159.99, 161.90, 165.67; **MS**, m/z: 432.18 (M^+, 36.61 %), 434.31 [$(M+2)^+$, 55.20%]; Anal. Calcd. For $C_{26}H_{16}N_4O_3$ (432.12): C, 72.21; H, 3.73; *N, 12.96; Found: C, 72.35; H, 3.90; N, 13.24.*

2.1.5.4.2-Amino-6-(4-(1,3-dioxoisoindolin-2-yl)phenyl)-4-(furan-2-yl) nicotinonitrile (13). **Yield** 75%; **m.p.** 330 - 332 °C; **IR** (KBr, cm^{-1}): 3420, 3347 (NH_2), 2208 (C≡N), 1716, 1660 (2C=O), 1599 (C=N), 1557 (C=C); **^{1}H NMR** (DMSO-d_6) δ (ppm): 6.16 (s, 2H, NH_2; exchangeable with D_2O), 6.79 – 6.82 (m, H, H_4 Ar`-H), 7.04 (d, H, $H_5$ Ar`-H), 7.56 (d, H, H_3 Ar`-H), 7.61 (d, $H_{2,6}$ Ar-H, *J* = 8.4 Hz), 7.83 (s, H, pyridine-H), 7.92 – 8.04 (m, 4H, Phthalimide-Hs), 8.26 (d, 2H, $H_{3,5}$ Ar-H, *J* = 8.4 Hz); **^{13}C NMR** (DMSO-d_6) δ (ppm): 105.07, 107.21, 113.29, 113.73, 117.68, 123.96, 127.69, 128.00, 132.00, 133.97, 135.27, 141.90, 149.16, 155.08, 158.44, 162.79, 167.33; **MS**, m/z: 406.32 (M^+, 100 %), 407.27 [$(M+1)^+$, 30.28%], 408.25 [$(M+2)^+$, 7.29%]; Anal. Calcd. For $C_{24}H_{14}N_4O_3$ (406.11): C, 70.93; H, 3.47; N, 13.79; Found: C, 71.08; H, 3.68; N, 13.88.

4.1.6. *General procedure for the synthesis of 6-(4-(1,3-Dioxoisoindolin-2-yl)phenyl)-2-oxo-4-(aryl)-1,2-dihydro pyridine-3-carbonitriles **(14-17)***

A mixture of 9 (2.65g, 0.01 mol), different aryl aldehydes (0.01 mol), ammonium acetate (6.16g, 0.08 mol) and ethyl cyanoacetate (1.13g, 0.01 mol) were refluxed in glacial acetic acid (15 ml) for 12 h. After completion of reaction, it was further cooled and filter the solid. The solid was purified by ethanol with 63 - 91% yields.

4.1.6.1.6-(4-(1,3-Dioxoisoindolin-2-yl)phenyl)-2-oxo-4-(p-tolyl)-1,2-dihydropyridine-3-carbonitrile (14). **Yield** 63%; **m.p.** 260 - 262 °C; **IR** (KBr, cm^{-1}): 3300 (NH) , 2222 (C≡N), 1720, 1680, 1665 (3C=O), 1614 (C=C); **^{1}H NMR** (DMSO-d_6) δ (ppm): 2.42 (s, 3H, CH_3-Hs), 6.98 (d, 2H, $H_{3,5}$ Ar`-H, *J* = 6 Hz), 7.09 (d, 2H, $H_{2.6}$ Ar`-H, *J* = 6 Hz), 7.35 (d, 2H, $H_{2,6}$ Ar-H, *J* = 8.4 Hz), 7.54 – 7.81 (m, 4H, Phthalimide-Hs), 8.00 (s, H, pyridine-H), 8.29 (d, 2H, $H_{3,5}$ Ar-H, *J* = 8.4 Hz), 10.31 (s, H, NH; exchangeable with D_2O); **^{13}C NMR** (DMSO-d_6) δ (ppm): 22.02, 99.98, 116.08, 117.93, 123.55, 124.65, 126.02, 127.67, 128.28, 130.93, 132.55, 133.13, 135.94, 137.02, 157.63, 159.56, 161.21, 167.44; **MS**, m/z: 431.42 (M^+, 33.55 %), 432.40 [$(M+1)^+$, 8.76%], 433.44 [$(M+2)^+$, 8.72%]; Anal. Calcd. For $C_{27}H_{17}N_3O_3$ (431.13): C, 75.16; H, 3.97; N, 9.74; Found: C, 75.37; H, 4.28; N, 9.81.

4.1.6.2.6-(4-(1,3-Dioxoisoindolin-2-yl)phenyl)-4-(4-methoxyphenyl)-2-oxo-1,2-dihydropyridine-3-carbonitrile (15). **Yield** 90%; **m.p.** 253 - 255 °C; **IR** (KBr, cm^{-1}): 3320 (NH) , 2218 (C≡N), 1718, 1689, 1663 (3C=O), 1602 (C=C); **^{1}H NMR** (DMSO-d_6) δ (ppm): 3.88 (s, 3H, CH_3O-Hs), 7.04 (d, 2H, $H_{3,5}$ Ar`-H, *J* = 8.4 Hz), 7.15 (d, 2H, $H_{2,6}$Ar`-H, *J* = 8.4 Hz), 7.63 (d, 2H, $H_{2,6}$ Ar-H, *J* = 8.4 Hz), 7.88 – 8.01 (m, 4H, Phthalimide-Hs), 8.10 (d, 2H, $H_{3,5}$ Ar-H, *J* = 8.4 Hz), 8.32 (s, H, pyridine-H), 10.39 (s, H, NH; exchangeable with D_2O); **^{13}C NMR** (DMSO-d_6) δ (ppm): 55.99,

99.70, 114.55, 115.98, 116.55, 123.39, 124.02, 127.50, 129.24, 131.97, 133.07, 134.78, 135.32, 136.29, 136.49, 157.85, 159.88, 161.98, 167.11; **MS**, m/z: 447.71 (M^+, 8.38 %); Anal. Calcd. For $C_{27}H_{17}N_3O_4$ (447.12): C, 72.48; H, 3.83; N, 9.39; Found: C, 72.90; H, 3.71; N, 9.48.

*4.1.6.3.6-(4-(1,3-Dioxoisoindolin-2-yl)phenyl)-4-(2-hydroxyphenyl)-2-oxo-1,2-dihydropyridine-3-carbonitrile (**16**).* **Yield** 85%; **m.p.** 181 - 183 ^oC; **IR** (KBr, cm^{-1}): 3429, 3201 (OH, NH) , 2220 (C≡N), 1709, 1699, 1667 (2C=O), 1601 (C=C); **^{1}H NMR** (DMSO-d_6) δ (ppm): 6.94 – 6.99 (m, 2H, $H_{3,5}$ Ar`-H), 7.27 - 7.36 (m, 2H, $H_{4,6}$ Ar`-H), 7.50 (d, $H_{2,6}$ Ar-H, J = 8.4 Hz), 7.87 (d, H, $H_{3,5}$ Ar-H, J = 8.4 Hz), 7.99 – 8.01 (m, 4H, Phthalimide-Hs), 8.29 (s, H, pyridine-H), 10.00, 10.99 (2s, 2H, OH, NH; exchangeable with D_2O); **^{13}C NMR** (DMSO-d_6) δ (ppm): 100.02, 116.70, 117.37, 117.72, 121.74, 123.39, 123.92, 124.74, 126.06, 126.46, 126.72, 129.05, 130.74, 132.01, 132.32, 133.07, 156.37, 158.95, 160.70, 165.34, 167.44; **MS**, m/z: 433.60 (M^+, 1.92 %), 434.31 [$(M+1)^+$, 0.85 %]; Anal. Calcd. For $C_{26}H_{15}N_3O_4$ (433.11): C, 72.05; H, 3.49; N, 9.70; Found: C, 72.31; H, 3.72; N, 9.89.

*4.1.6.4.6-(4-(1,3-dioxoisoindolin-2-yl)phenyl)-4-(furan-2-yl)-2-oxo-1,2-dihydropyridine-3-carbonitrile (**17**).* **Yield** 91%; **m.p.** 150 - 152^oC; **IR** (KBr, cm^{-1}): 3356 (NH) , 2221 (C≡N), 1716, 1695, 1650 (3C=O), 1596 (C=C); **^{1}H NMR** (DMSO-d_6) δ (ppm): 6.90 – 7.08 (m, H, $H_{3,4}$ Ar`-H), 7.26 (d, $H_{2,6}$ Ar-H, $J$ = 8.4 Hz), 7.59 – 7.73 (m, 4H, Phthalimide-Hs), 7.83 ( s, H, pyridine-H), 7.91 (d, H, $H_5$ Ar`-H), 8.26 (d, 2H, $H_{3,5}$ Ar-H, J = 8.4 Hz), 10.48 (s, 2H, NH_2; exchangeable with D_2O); **^{13}C NMR** (DMSO-d_6) δ (ppm): 97.37, 110.73, 114.80, 115.75, 121.34, 123.56, 125.13, 126.04, 127.56, 131.25, 132.37, 135.65, 139.59, 148.65, 159.27, 162.68, 167.36, 169.55; **MS**, m/z: 407.28 (M^+, 42.70 %); Anal. Calcd. For $C_{24}H_{13}N_3O_4$ (407.09): C, 70.76; H, 3.22; N, 10.31; Found: C, 70.94; H, 3.41; N, 10.58.

4.2. Biological evaluation

4.2.1. Anticancer screening

Cancer cells from different cancer cell lines; Human prostate carcinoma cell lines (PC-3), hepatocellular carcinoma cell lines (HEPG-2) and human breast adenocarcinoma cell line (MCF-7) were obtained from American Type Cell Culture Collection (ATCC, Manassas, USA) and grown on the appropriate growth medium Dulbecco's modified Eagle's medium (DMEM/Life Technologies) supplemented with 10% FBS (fetal bovine serum) (Hyclone), 10 ug/ml of insulin (Sigma) and 1% penicillin–streptomycin. All the other chemicals and reagents were from Sigma, or Invitrogen. Plate cells (cells density 1.2 – 1.8 _ 10,000 cells/well) in a volume of 100 ml complete growth medium + 100 ul of the tested compound per well in a 96-well plate for 24 h before the MTT assay.

4.2.2. PIM-1 kinase inhibitory activity

The effects of the synthesized compounds **6, 7, 8, 12** and **13** on the activity of PIM-1 kinase were measured using Human proto-oncogene serine/threonine- protein kinase PIM-1 (PIM-1) ELISA Kit (catalog #MBS701210). The cells were centrifuged for 15 min at 1000x g, 2-8℃ and assayed immediately according to the manufacturer's instructions. Shortly, the assay was performed using 100 mL of the supernatant of the cell, which were incubated for 2 h at 37℃ before starting the assay procedure. Finally, the optical density of each well was determined within 5 min using a microplate reader set at 450 nm.

4.2.3. Cell cycle analysis

PC-3 cells were seeded in a 6-well plate at a concentration of 1×10^5 cells per well, then incubated for 24 h. The cells were treated with (0.1% DMSO) vehicle or 2.04 µM of **6, 7, 8, 12** and **13** compounds for 24 h. After that, cells were harvested and fixed for 12 h using ice-cold 70% ethanol at 4 °C. Removal of ethanol and washing cells with cold PBS was done; then, incubated for 30 min at 37 °C in 0.5 ml of PBS containing 1 mg/mL Rnase. The cells were stained for 30 min with propidium iodide in the dark. Then flow cytometer was used to detect DNA contents. [43]

4.2.4. Annexin V-FITC apoptosis assay

PC-3 cells were seeded in a 6-well plate ($1 X10^5$ cell/well), incubated for 24 h; then treated with vehicle (0.1% DMSO) or 2.04 µM of compounds **6, 7, 8, 12** and **13** for 24 h. The cells were then harvested, washed using PBS and stained for 15 min at room temperature in the dark using annexin V-FITC and PI in binding buffer (10 mM HEPES, 140 mM NaCl, and 2.5 mM CaCl2 at pH 7.4), then analyzed by the flow cytometer. [44]

4.2.5. Apoptosis studies

4.2.5.1. Effects on the level of active caspase 3

To determine the effect of **6, 7, 8, 12** and **13** on apoptosis, the active caspase 3 level was measured by using Quantikine-Human active Caspase 3 Immunoassay (R&D Systems, Inc. Minneapolis, USA) according to the manufacturer protocol. Briefly, after washing the cells with PBS, the cells were collected and lysed by adding it to the extraction buffer containing protease inhibitors (1 mL per 1 x 107 cells.) then the lysate was diluted immediately before the assay. At the end of the assay the optical density of each well was determined within 30 min using a microplate reader set at 450 nm.

4.2.5.2. Effects on mitochondrial apoptosis pathway proteins Bax and Bcl-2

Cells were obtained from American Type Culture Collection, cells were grown in RPMI 1640 containing 10% fetal bovine serum at 37°C, stimulated with the compounds to be tested for BAX or Bcl-2 and lysed with Cell Extraction Buffer. This lysate was diluted in Standard Diluent Buffer over the range of the assay and measured for human active BAX or Bcl-2 content. (cells

are Plated in a density of 1.2 – 1.8 × 10,000 cells/well in a volume of 100µl complete growth medium + 100 ul of the tested compound per well in a 96-well plate for 24 hours before measured for human active BAX or Bcl-2).

4.3. Molecular modeling and in silico predictions

4.3.1. Molecular docking study

The molecular modeling study was performed using the Molecular Operating Environment (MOE 2010) software. The three-dimensional structures and conformations of the enzymes were acquired from the Protein Data Bank (PDB) website using PIM-1 kinase (PDB ID code 2OBJ). The ligand molecules were constructed in MOE using the builder module and collected in a database. The database was prepared by using the option "Protonate 3D" to add hydrogens, calculate partial charges and minimize energy (using Force Field MMFF94x). In addition, the protein structure was prepared by deleting the repeated chains, water molecules and any surfactants, hydrogens were also added to the atom of the receptor and the partial charges were calculated. MOE was used to calculate the best score between the ligands and the enzymes' binding sites. Scoring was determined using alpha HB as a scoring function. The resulted database contained the score between the ligands' conformers and the enzyme binding sites in kcal/mol. To confirm the credibility of docking results, self-docking was used to validate the adopted docking protocol in which co-crystallized ligand (VRV) were drawn in MOE, prepared as the targeted compounds (hydrogens addition, partial charges calculation and energy minimization), and then docked into the active site of the protein using the same protocol. The top ranked pose exhibited Root mean square deviation (RMSD) value of less than 1.5 Å from the experimental crystal structure. This result indicated that the Molecular Operating Environment (MOE) docking could reliably predict docking pose for the studied compounds to an enzyme. It was reported that values less than 1.5 or 2 Å were a sign of a successful and reliable docking protocol.

4.3.2. *In silico prediction of physicochemical and ADME properties and pharmacokinetic profile*

Compounds **6**, **7**, **8**, **12** and **13** were subjected to molecular properties prediction by Molinspiration online property calculation toolkit, drug-likeness, and solubility parameter calculation by MolSoft software, ADME profiling by Pre-ADMET calculator. Toxicity risk assessment and Ligand efficiency metrics calculation by Data warrior software. Pgp substrate, bioavailability score and synthetic accessibility prediction were evaluated by SWISSADME online website. While PAINS prediction was performed by SWISSADME online website and PAINS-Remover, to evaluate and analyse their suitability to qualify for a drug candidate.

Declaration of competing interest

Authors have no conflict of interest to declare.

References

[1] G.M. Arunesh, E. Shanthi, M.H. Krishna, J. Sooriya Kumar, V.N. Viswanadhan, Small molecule inhibitors of PIM1 kinase: July 2009 to February 2013 patent update, Expert Opin. Ther. Pat. 24 (2014) 5–17. https://doi.org/10.1517/13543776.2014.848196.

[2] L. Brault, C. Gasser, F. Bracher, K. Huber, S. Knapp, J. Schwaller, Pim serine/threonine kinases in the pathogenesis and therapy of hematologic malignancies and solid cancers, Haematologica. 95 (2010) 1004–1015. https://doi.org/10.3324/haematol.2009.017079.

[3] D. Drygin, M. Haddach, F. Pierre, D.M. Ryckman, Potential use of selective and nonselective pim kinase inhibitors for cancer therapy, J. Med. Chem. 55 (2012) 8199–8208. https://doi.org/10.1021/jm3009234.

[4] S. Guo, X. Mao, J. Chen, B. Huang, C. Jin, Z. Xu, S. Qiu, Overexpression of Pim-1 in bladder cancer, J. Exp. Clin. Cancer Res. 29 (2010) 1–7. https://doi.org/10.1186/1756-9966-29-161.

[5] A.L. Merkel, E. Meggers, M. Ocker, PIM1 kinase as a target for cancer therapy, Expert Opin. Investig. Drugs. 21 (2012) 425–436. https://doi.org/10.1517/13543784.2012.668527.

[6] T. Morwick, Pim kinase inhibitors: A survey of the patent literature, Expert Opin. Ther. Pat. 20 (2010) 193–212. https://doi.org/10.1517/13543770903496442.

[7] M.C. Nawijn, A. Alendar, A. Berns, For better or for worse: The role of Pim oncogenes in tumorigenesis, Nat. Rev. Cancer. 11 (2011) 23–34. https://doi.org/10.1038/nrc2986.

[8] B.T. Le, M. Kumarasiri, J.R.J. Adams, M. Yu, R. Milne, M.J. Sykes, S. Wang, Targeting Pim kinases for cancer treatment: Opportunities and challenges, Future Med. Chem. 7 (2015) 35–53. https://doi.org/10.4155/fmc.14.145.

[9] M. Narlik-Grassow, C. Blanco-Aparicio, A. Carnero, The PIM family of serine/threonine kinases in cancer, Med. Res. Rev. 34 (2014) 136–159.

[10] Y. Tursynbay, J. Zhang, Z. Li, T. Tokay, Z. Zhumadilov, D. Wu, Y. Xie, Pim-1 kinase as cancer drug target: An update (Review), Biomed. Reports. 4 (2016) 140–146. https://doi.org/10.3892/br.2015.561.

[11] W. Zhao, R.Y. Qiu, P. Li, J. Yang, PIM1: a promising target in patients with triple-negative breast cancer, Med. Oncol. 34 (2017). https://doi.org/10.1007/s12032-017-0998-y.

[12] J. Li, B.E. Loveland, P.X. Xing, Anti-Pim-1 mAb inhibits activation and proliferation of T lymphocytes and prolongs mouse skin allograft survival, Cell. Immunol. 272 (2011) 87–93. https://doi.org/10.1016/j.cellimm.2011.09.002.

[13] N.A. Warfel, A.S. Kraft, PIM kinase (and Akt) biology and signaling in tumors,

Pharmacol. Ther. 151 (2015) 41–49. https://doi.org/10.1016/j.pharmthera.2015.03.001.

[14] Y. XIE, S. BAYAKHMETOV, PIM1 kinase as a promise of targeted therapy in prostate cancer stem cells, Mol. Clin. Oncol. 4 (2016) 13–17. https://doi.org/10.3892/mco.2015.673.

[15] M. Bachmann, H. Hennemann, X.X. Pei, I. Hoffmann, T. Möröy, The oncogenic serine/threonine kinase Pim-1 phosphorylates and inhibits the activity of Cdc25C-associated kinase 1 (C-TAK1): A Novel role for Pim-1 at the G2TM cell cycle checkpoint, J. Biol. Chem. 279 (2004) 48319–48328. https://doi.org/10.1074/jbc.M404440200.

[16] T. Hirano, K. Ishihara, M. Hibi, Roles of STAT3 in mediating the cell growth, differentiation and survival signals relayed through the IL-6 family of cytokine receptors, Oncogene. 19 (2000) 2548–2556. https://doi.org/10.1038/sj.onc.1203551.

[17] L.T. Lam, H. Zhang, J. Xue, P. Hessler, S.K. Tahir, J. Chen, S. Jin, A.J. Souers, J.D. Leverson, Colorectal cancer cell lines with high BCL-XL and low MCL-1 expression are sensitive to a potent and selective BCL-XL inhibitor, (2014).

[18] M.M.F. Ismail, A.M. Farrag, M.F. Harras, M.H. Ibrahim, A.B.M. Mehany, Bioorganic Chemistry Apoptosis : A target for anticancer therapy with novel cyanopyridines, Bioorg. Chem. 94 (2020) 103481. https://doi.org/10.1016/j.bioorg.2019.103481.

[19] R.K. Yadlapalli, O.P. Chourasia, M.P. Jogi, A.R. Podile, R.S. Perali, Design, synthesis and in vitro antimicrobial activity of novel phenylbenzamido-aminothiazole-based azasterol mimics, Med. Chem. Res. 22 (2013) 2975–2983. https://doi.org/10.1007/s00044-012-0314-5.

[20] O.M. Abdel Hafez, M.I. Nassar, S.M. El-Kousy, A.F. Abdel-Razik, S.M.M. Atalla, M.M. El-Ghonemy, Synthesis of some new carbonitriles and pyrazole coumarin derivatives with potent antitumor and antimicrobial activities, Acta Pol. Pharm. - Drug Res. 71 (2014) 593–601.

[21] A. Malki, M. Mohsen, H. Aziz, O. Rizk, O. Shaaban, M. El-Sayed, Z.A. Sherif, H. Ashour, New 3-cyano-2-substituted pyridines induce apoptosis in MCF 7 breast cancer cells, Molecules. 21 (2016) 1–25. https://doi.org/10.3390/molecules21020230.

[22] H.H. Eissa, Synthesis of bisphthaldicarboximide via the reaction of phthalic anhydride with diamines and evaluation of its biological activity., Int. J. ChemTech Res. 6 (2014) 95–101, 7 pp. http://sphinxsai.com/2014/ChemTech/JM14CT1_50/CT=11(95-101)JM14.pdf.

[23] I. Abbas, S. Gomha, M. Elaasser, M. Bauomi, Synthesis and biological evaluation of new pyridines containing imidazole moiety as antimicrobial and anticancer agents, Turkish J. Chem. 39 (2015) 334–346. https://doi.org/10.3906/kim-1410-25.

[24] P. Prayong, S. Barusrux, N. Weerapreeyakul, Cytotoxic activity screening of some indigenous Thai plants, Fitoterapia. 79 (2008) 598–601.

https://doi.org/10.1016/j.fitote.2008.06.007.

[25] I.W. Cheney, S. Yan, T. Appleby, H. Walker, T. Vo, N. Yao, R. Hamatake, Z. Hong, J.Z. Wu, Identification and structure-activity relationships of substituted pyridones as inhibitors of Pim-1 kinase, Bioorganic Med. Chem. Lett. 17 (2007) 1679–1683. https://doi.org/10.1016/j.bmcl.2006.12.086.

[26] T. Rudel, Caspase inhibitors in prevention of apoptosis, Herz. 24 (1999) 236–241. https://doi.org/10.1007/BF03044967.

[27] S. Fulda, L. Galluzzi, G. Kroemer, Targeting mitochondria for cancer therapy, Nat. Rev. Drug Discov. 9 (2010) 447–464. https://doi.org/10.1038/nrd3137.

[28] S. Salakou, D. Kardamakis, A.C. Tsamandas, V. Zolota, E. Apostolakis, V. Tzelepi, P. Papathanasopoulos, D.S. Bonikos, T. Papapetropoulos, T. Petsas, D. Dougenis, Increased bax/bcl-2 ratio up-regulates caspase-3 and increases apoptosis in the thymus of patients with Myasthenia gravis, In Vivo (Brooklyn). 21 (2007) 123–132.

[29] N.Ö. Can, D. Osmaniye, S. Levent, B.N. Sağlık, B. Korkut, Ö. Atlı, Y. Özkay, Z.A. Kaplancıklı, Design, synthesis and biological assessment of new thiazolylhydrazine derivatives as selective and reversible hMAO-A inhibitors, Eur. J. Med. Chem. 144 (2018) 68–81. https://doi.org/10.1016/j.ejmech.2017.12.013.

[30] E. Rajanarendar, S. Rama Krishna, D. Nagaraju, K. Govardhan Reddy, B. Kishore, Y.N. Reddy, Environmentally benign synthesis, molecular properties prediction and anti-inflammatory activity of novel isoxazolo[5,4-d]isoxazol-3-yl-aryl-methanones via vinylogous Henry nitroaldol adducts as synthons, Bioorganic Med. Chem. Lett. 25 (2015) 1630–1634. https://doi.org/10.1016/j.bmcl.2015.01.041.

[31] D.F. Veber, S.R. Johnson, H.Y. Cheng, B.R. Smith, K.W. Ward, K.D. Kopple, Molecular properties that influence the oral bioavailability of drug candidates, J. Med. Chem. 45 (2002) 2615–2623. https://doi.org/10.1021/jm020017n.

[32] Molinspiration Cheminformatics, (n.d.). https://www.molinspiration.com/ (accessed June 15, 2020).

[33] Molsoft L, (n.d.).

[34] PreADMET | Prediction of ADME/Tox – Just another BMDRC Sites site, (n.d.). https://preadmet.bmdrc.kr/ (accessed June 15, 2020).

[35] www.openmolecules.org, (n.d.). http://www.openmolecules.org/datawarrior/ (accessed June 15, 2020).

[36] J.B. Baell, G.A. Holloway, New substructure filters for removal of pan assay interference compounds (PAINS) from screening libraries and for their exclusion in bioassays, J. Med. Chem. 53 (2010) 2719–2740. https://doi.org/10.1021/jm901137j.

[37] A. Daina, O. Michielin, V. Zoete, SwissADME: A free web tool to evaluate pharmacokinetics, drug-likeness and medicinal chemistry friendliness of small molecules, Sci. Rep. 7 (2017) 1–13. https://doi.org/10.1038/srep42717.

[38] Y.H. Zhao, M.H. Abraham, J. Le, A. Hersey, C.N. Luscombe, G. Beck, B. Sherborne, I. Cooper, Rate-limited steps of human oral absorption and QSAR studies, Pharm. Res. 19 (2002) 1446–1457. https://doi.org/10.1023/A:1020444330011.

[39] N. Kumar, R. Tomar, A. Pandey, V. Tomar, V.K. Singh, R. Chandra, Preclinical evaluation and molecular docking of 1,3-benzodioxole propargyl ether derivatives as novel inhibitor for combating the histone deacetylase enzyme in cancer, Artif. Cells, Nanomedicine Biotechnol. 46 (2018) 1288–1299. https://doi.org/10.1080/21691401.2017.1369423.

[40] J.L. Dahlin, J.W.M. Nissink, J.M. Strasser, S. Francis, L. Higgins, H. Zhou, Z. Zhang, M.A. Walters, PAINS in the assay: Chemical mechanisms of assay interference and promiscuous enzymatic inhibition observed during a sulfhydryl-scavenging HTS, J. Med. Chem. 58 (2015) 2091–2113. https://doi.org/10.1021/jm5019093.

[41] J. Baell, M.A. Walters, Chemistry: Chemical con artists foil drug discovery, Nature. 513 (2014) 481–483. https://doi.org/10.1038/513481a.

[42] D. Döpp, A.A. Hassan, A.F.E. Mourad, A.M. Nour El-Din, K. Angermund, C. Krüger, C.W. Lehmann, J. Rust, New reaction of ethenetetracarbonitrile with N-arylisoindolines, Tetrahedron. 59 (2003) 5073–5081. https://doi.org/10.1016/S0040-4020(03)00735-X.

[43] J. Wang, M.J. Lenardo, Roles of caspases in apoptosis, development, and cytokine maturation revealed by homozygous gene deficiencies, J. Cell Sci. 113 (2000) 753–757.

[44] K.K.W. Lo, T.K.M. Lee, J.S.Y. Lau, W.L. Poon, S.H. Cheng, Luminescent biological probes derived from ruthenium(II) estradiol polypyridine complexes, Inorg. Chem. 47 (2008) 200–208. https://doi.org/10.1021/ic701735q.

.

Highlights

- Synthesized of new 14 6-(4-benzamido-/4-phthalimido)-3-cyanopyridine derivatives.
- Cytotoxicity of all the new derivatives is given and discussed.
- PIM-1 kinase inhibitory activity were evaluated for the most five active derivatives.
- Apoptosis studies and cell cycle analysis were evaluated for the most five active derivatives.
- Molecular modelling of the most active compound with PIM-1 kinase enzyme was done
- *In silico* assessment of the most five active derivatives pharmacokinetic was performed.

Declaration of interests

☒ The authors declare that they have no known competing financial interests or personal relationships that could have appeared to influence the work reported in this paper.

☐The authors declare the following financial interests/personal relationships which may be considered as potential competing interests: